Mechanics & Industry **24**, 31 (2023)
© J. Li et al., Published by EDP Sciences 2023
https://doi.org/10.1051/meca/2023020

Mechanics & Industry

Available online at:
www.mechanics-industry.org

REGULAR ARTICLE OPEN ACCESS

Inertia matching of CNC cycloidal gear form grinding machine servo system

Jubo Li[1,2], Jianxin Su[1,2], Ming Gao[3], Donghui Zhao [4], Leilei Zhang [3], Dinghe Wang[4], and Fusheng Shi[4]

[1] School of Mechatronics Engineering, Henan University of Science and Technology, Luoyang, Henan 471003, PR China
[2] Advanced manufacturing of mechanical equipment Henan Collaborative Innovation Center, Henan University of Science and Technology, Luoyang, Henan 471003, PR China
[3] First Tractor Company Limited, Luoyang, Henan 471004, PR China
[4] Zhong Bang Superhard tools Co. Ltd, Zhengzhou, Henan 450001, PR China

Received: 9 September 2022 / Accepted: 14 June 2023

Abstract. Reasonable ratio between the load inertia and servo motor inertia plays a decisive role for the dynamic performance and stability of the servo system, as well as the machining accuracy of the whole CNC machine. In order to improve the control performance and contour machining accuracy of the servo system of the CNC cycloidal gear form grinding machine, an optimization design method of the inertia matching for the CNC cycloidal gear form grinding machine servo system is proposed. The two-mass servo driving closed-loop PID control system is constructed, the influence of the different inertia ratios on the dynamic performance and contour errors of the servo system are deeply analyzed, and the inertia ratio is optimized to satisfied with the servo system performance requirements. Finally, the feasibility and practicability of the optimization design method of inertia matching are verified through the inertia ratio optimization grinding experiments of the cycloid gear in the CNC gear form grinding machine. This inertia matching optimization design method provides a valuable reference for the further design of CNC machine servo system.

Keywords: Servo system / CNC cycloidal gear form grinding machine / inertia matching / inertia ratio

1 Introduction

With the rapid development of the numerical control and computer technologies, the modern precision grinding technology has put forward more requirements for the computer numerical control (CNC) gear grinding machine, such as more sensitive response, higher motion precision, and stronger reliability. After being manufactured, the entire operation performance of the CNC gear grinding machine usually needs to be test. If the test is conducted directly on the machine, it is not only low efficiency, but also may cause damage even safety accidents to the machine due to the unreasonable parameter settings. In the practical engineering application, the ratio of the load inertia to servo motor inertia is very important for the CNC gear grinding machine servo system. If the ratio of inertia exceeds reasonable control range, the servo system may generate oscillation or control failure, which will have a direct effect on the dynamic performance, stability, and machining accuracy of the servo system.

The CNC cycloidal gear form grinding machine is a key CNC equipment to realize the high-efficiency and high-precision grinding of the rotary vector reducer cycloid gear. Therefore, it is urgent to carry on the inertia matching design of the CNC cycloidal gear form grinding machine so as to keep the inertia ratio within an appropriate range, which not only guarantees the fast response and stable operation of the servo driving system, but also satisfies the ideal geometric accuracy of the gear machining. Aiming at the inertia matching design of the CNC machine, relevant scholars at home and abroad have carried out relevant research.

For instance, Richard [1] analyzed and demonstrated the Kolmorgen motor with known torque, and concluded through mathematical formula derivation and experiment that when the inertia ratio of load was set to 1, the feed system could obtain the maximum load acceleration capacity. Li et al. [2] studied the speed adaptive control technology of the permanent magnet synchronous motor system with varied load inertia. Zhang and Furusho [3] studied the dynamic performance of a two-mass system with different inertia ratios by using three pole assignment methods. Younkin et al. [4] concluded through theoretical

* e-mail: 9903437@haust.edu.cn

analysis and experiments that reducing the moment of inertia of the motor shaft would not only affect the acceleration performance and followability of the system, but also affect the robustness of the controller, system bandwidth, dynamic stiffness, etc. Pritschow [5] used the motor-load isolation single inertia-spring model to give the approximate relationship between the load mass and the upper limit of control gain and anti-jamming stiffness, and pointed out that increasing the load inertia will improve the anti-jamming ability. By means of closed-loop frequency response discussion, Moscrop et al. [6] analysed the effects of high motor-load inertia mismatch on servo system performance by using closed loop frequency responses. On this basis, presented the fast feedback control methods to improve the system response and verified the effectiveness of these control methods through the comprehensive experiment. Benath et al. [7] proposed a new design rule for servo driving applications to select a servo motor with an optimal energy transmission ratio. Boscariol et al. [8] proved that the most common size criteria based on inertia matching could not obtain the most energy-efficient design through the parameterized analysis based on motor size, deceleration ratio and inertia ratio, as well as the energy consumption analysis for each design sample.

Besides, Shao et al. [9] studied a parallel robot, comprehensively considered the resonance frequency, acceleration torque and dynamic performance of the machine tool, and combined with simulation, obtained the inertia index and the appropriate matching range of inertia, which has been popularized and applied. Zhang et al. [10] proposed a new method to study the design law of inertia ratio. By eliminating the influence of servo control, they studied the matching characteristics of motion process and inertia ratio under high speed and high acceleration, and proved that the inertia ratio must be strictly limited within a certain range to effectively improve the system performance, which provided theoretical support for the design of high-speed machine tools. Zhang et al. [11] researched on the effect of load inertia on system performance and contour errors of 5-coordinate cross beam mobile gantry machining center in time and frequency domain, and provided a reasonable selection range of inertia ratio of CNC machine tools in different machining forms, which provided theoretical basis for the inertia matching of heavy CNC machine tools. Liu et al. [12] employed the dual inertia model to analyze the relationship between energy matching efficiency and inertia ratio, and put forward the general design steps and basic methods of the load inertia ratio of servo system. Yuan et al. [13] proposed a method to obtain the positioning accuracy and synchronization control accuracy of servo motion system. Wang et al. [14] took servo motor selection of three-axis transmission system in a CNC machine tools for example, established a servo motor selection mathematical model of transmission system in CNC machine tool, deeply analyzed the parameter selection and calculation of horizontal, inclined and vertical transmission system, and proved the rationality of the method by engineering test and motor control software.

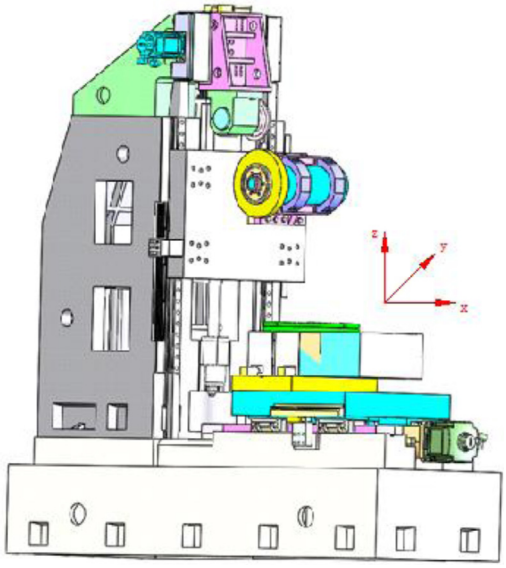

Fig. 1. Designed YK7350B form grinding machine model.

All of the above researches have obtained very important research results, which provide the theory and foundation for the inertia matching research of servo system. However, there have been few scholars or actual papers that have studied the inertia matching technology of CNC cycloidal gear form grinding machine servo system.

In view of this, an optimization design method of inertia matching for the CNC cycloidal gear form grinding machine servo system is proposed to improve its control performance and contour machining accuracy in this paper. The closed-loop PID control system of two-mass servo driving is constructed, the dynamic performance of the single-axis driving system and the double-axes driving system under different inertia ratios are compared, and the influence of inertia ratio on the servo system contour errors under the double-axes simultaneous control is analyzed. Finally, the inertia ratio satisfying the servo system performance requirements is optimized, and the feasibility and practicability of the optimization design method of inertia matching are verified through the inertia ratio optimization grinding experiments of the cycloid gear in the CNC gear form grinding machine.

2 Design and optimization of servo system inertia matching

According to the actual CNC machining needs of cycloidal gear, the designed YK7350B form grinding machine model and the form grinding model of the cycloidal gear are shown in Figures 1 and 2, respectively.

In Figure 2, *Oxyz* is the right-hand Cartesian coordinate system, the subscript "*J*" represents the coordinate system of grinding wheel dressing wheel, subscript "G" indicates grinding wheel coordinate system, and subscript "2" indicates the workpiece coordinate system. "E" refers to the distance between the center of grinding wheel and the center of cycloidal gear in the workpiece moving direction.

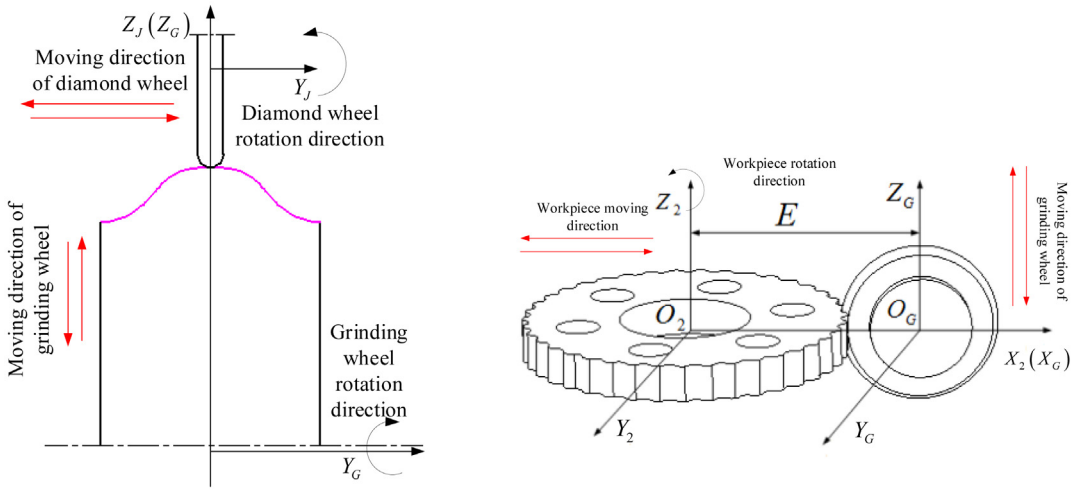

Fig. 2. Form grinding model of cycloidal gear.

Table 1. X-axis and Z-axis design parameters of gear forming machine YK7350B.

Structural parameters	Axis X	Axis Z
Lead screw length	1.5 m	1.2 m
Lead screw diameter	0.04 m	0.04 m
Lead screw double driving span	1.9 m	0.8 m
Servo torque	15.86/2 N m	11.73/2 N m
Rotor inertia	75/2 kg. cm^2	56/2 kg. cm^2
Initial load inertia	371 kg. cm^2	260 kg. cm^2

X-axis and Z-axis are the two servo driving axes of the cycloidal gear form grinding. In the cycloidal gear grinding processing, the corresponding machining motion is mainly completed through the coordination of X-axis and Z-axis, and the relevant design parameters of each axis are shown in Table 1.

According to the different inertia ratios of cycloidal gear grinding machines and their dynamics relationships, the simulation analysis model is built to analyze the step response, gain upper limit, following error, frequency characteristics and anti-interference stiffness of the single-axis double-driving servo system and the single-axis single-driving servo system under different inertia ratios. At the same time, when the X-axis and Z-axis are simultaneously controlled, the influence laws of different inertia ratios on the contour errors of the two-axis simultaneous motion can be analyzed, and then the accurate inertia ratio range can be optimized under the premise of meeting various performance requirements.

2.1 Inertia matching design of servo system

In the design of CNC cycloidal gear form grinding machine, it can be obtained that the weight of the load (including workbench and workpiece) of the CNC cycloidal gear form grinding machines is about $m_1 = 300\,kg$, the friction coefficient between the sliding table and the guide rail is $\mu = 0.002$, and the pitch, diameter, weight of the ball screw are about $S = 26$mm , $D = 80$mm and $m_2 = 40kg$, respectively $\mu = 0.002$. Assume that the mechanical transmission efficiency is $\eta = 95\%$, the maximum moving speed of the sliding table is $v = 0.8$m/s, and the acceleration and deceleration time is $t = 0.5$.s. In the selection design and quantitative calculation of servo motor, the calculation of servo motor speed, torque required to overcome the friction, torque required for heavy acceleration, and torque required for screw acceleration are shown in equations (1)−(4), respectively.

$$n = v/S = 1846r/\text{min} \tag{1}$$

$$T_1 = \mu m_1 g \times S/(2\pi \times \eta) = 0.026\text{N·m} \tag{2}$$

$$T_2 = m_1 a \times S/(2\pi \times \eta) = 2.092\text{N·m} \tag{3}$$

$$T_3 = \frac{(m_2 D^2/8) \times (2\pi n/60)}{(t \times \eta)} = 13.74\text{N·m}. \tag{4}$$

According to equations (2)−(4), the maximum driven torque required for the motor is shown in equation (5).

$$T = T_1 + T_2 + T_3 = 15.86\text{N·}m \tag{5}$$

The maximum loading inertia converted to the motor shaft is shown in equation (6).

$$J_L = m_1 \times (S/2\pi)^2 + m_2 \times D^2/8 = 371.42\text{kg·cm}^2. \tag{6}$$

Thus, according to the structure design parameters of cycloidal gear grinding machine and the design parameters of CNC servo system, the corresponding parameters of servo motor can be preliminarily selected based on the servo motor selection manual, such as the rated speed is 2000 r/min, the rated torque is 16 N · m, and the rotor inertia is 75kg · cm^2. Theoretically, the loading inertia ratio of the motor can be calculated, which is about 371.42/75 ≈ 4.95 and satisfies the principle of inertia matching.

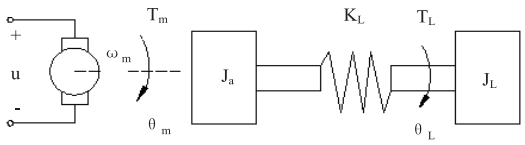

Fig. 3. Two-mass servo system model.

2.2 Servo system inertia matching optimization

In order to optimize the inertia matching, the concept of two-mass servo system is introduced and the two-mass servo driving closed-loop system is constructed for simulation analysis. Generally, the servo motors and loads are seen as a whole and called the single-mass servo system. However, for a real servo system, the rigidity of mechanical driving components is finite. Under the action of motor driving torque, the mechanical shaft will be deformed to some extent. in the qualitative calculation, the inertia of driving shaft J_a is usually added to the maximum load inertia on the motor shaft J_L to simplify the motor driving system into a two-mass servo system composed of motor and load [15]. The two-mass servo system model is shown in Figure 3.

In Figure 3, u is the power supply voltage, θ_{m} is the motor rotation angle, θ_{L} is the loading rotation angle, T_{m} is the motor torque, T_{L} is the load torque, J_a is the rotational inertia of the transmission shaft, J_L is the maximum load inertia on the motor shaft, and K_L is the coupling stiffness coefficient, and the servo motor control model of the two-mass servo system is shown in Figure 4.

According to Figure 4, the electric equation of the servo motor can be obtained, which is shown in equation (7).

$$\begin{aligned} iR + L\mathrm{i} = ua - C_{\mathrm{e}}\theta_{\,m} - K_i i\,T_m = iK_m J_m \theta_m \\ = T_m - b_m\theta_m - K_L(\theta_m - \theta_L) \end{aligned} \tag{7}$$

where, L is the armature inductance, R is the armature resistance, C_e is the motor viscous damping coefficient, K_{i} is the current feedback coefficient, K_{m} is the motor torque coefficient, b_m is the motor viscous damping coefficient, J_m is the motor inertia, J_L is the load inertia, and T_{d} is the disturbance torque which including the friction torque and coupling torque. Meanwhile, the load model of the two-mass servo system is shown in Figure 5.

According to Figure 5, the loading dynamics equation is shown in equation (8).

$$J_L\,\ddot{\theta}_L = T_{\mathrm{mL}} - b_L\dot{\theta}_L \qquad T_{\mathrm{mL}} = K_L(\theta_m - \theta L) \tag{8}$$

where, b_{L} is the loading viscous damping factor.

Combining equations (7) and (8), the loading motor inertia ratio can be obtained, which is shown in equation (9).

$$\begin{aligned} \frac{J_L}{J_m} = \frac{(R + L + K_i)(K_L\theta_m - K_L\theta_L - b_L\dot{\theta}_L)}{(u - C_e\dot{\theta}_m)K_m - (R + L + K_i)(b_m\dot{\theta}_m} \\ + K_L\theta_m - K_L\theta_L)\frac{\dot{\theta}_m}{\ddot{\theta}_L} \end{aligned} \tag{9}$$

According to Figures 3–5, the structural model of the motor-load two-mass servo system can be established, as shown in Figure 6. Meanwhile, the simulation model of the two-mass servo PID control system can be constructed with the help of the Simulink, which is shown in Figure 7.

3 Influences of the inertia ratio on the servo system control performances

In order to better match the inertia ratio of the designed servo system, the influence laws of the inertia ratio on the servo system performances (e.g., unit step response performance, upper limit of control gain, following error, anti-interference stiffness, and closed-loop frequency characteristics) are analyzed respectively.

3.1 Influence on the unit step response performance

The unit step response can directly reflect the dynamic performance of the servo system. The dynamic response characteristics of the servo system can be reflected by the parameters (e.g., delay time t_d, rise time t_x, peak time t_p, overshoot σ and adjustment time t_s) of the response curve. Where, t_x can reflect the sensitivity and the transient process speed of the servo system, σ can reflect the smoothness of the servo system transient process, t_s can reflect the damping and response speeds of the servo system. Due to the frequent startup and braking, acceleration and deceleration, the speediness and overshoot under the step signal response are the two important indicators for evaluating the dynamic performance of the servo system. The response curve of the servo system under the step signal is shown in Figure 8.

Under the same output torque T_{L}, the smaller the inertia of the mechanical structure, the greater the angular acceleration, and the faster the response speed of the servo system. For the second-order mechanical systems, the inherent frequency ω_n, the damping ratio ξ, the overshoot σ, and the adjustment time t_s can be expressed, which are shown in equations(10) and (11), respectively.

$$\begin{cases} w_n = \sqrt{\dfrac{K}{J}} \\ \xi = \dfrac{\mathrm{B_L}}{2\sqrt{KL}} \end{cases} \tag{10}$$

$$\begin{cases} \sigma = e^{-\dfrac{\xi\pi}{\sqrt{1 - W_n^2}}} \\ t_s \approx \dfrac{3}{\xi w_n^2} \end{cases} \tag{11}$$

According to equations (10) and (11), it is can be demonstrated that the damping of the system B_L is proportional to the damping ratio ξ, the smaller the damping $B_{L,}$ the longer the adjustment time of the servo system t_s, and the larger the overshoot σ. For the high-

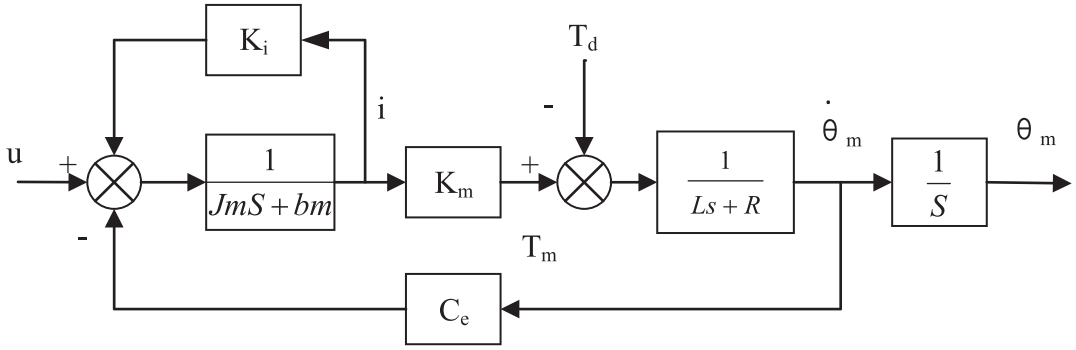

Fig. 4. Servo motor control model of the two-mass servo system.

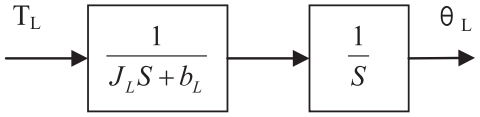

Fig. 5. Load model of the two-mass servo system.

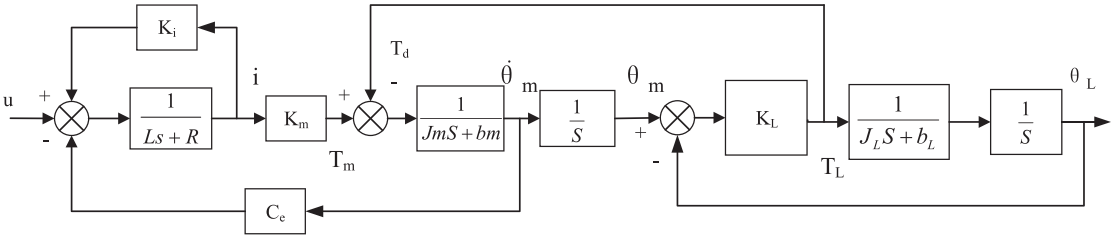

Fig. 6. Structural model of the motor-load two-mass servo system.

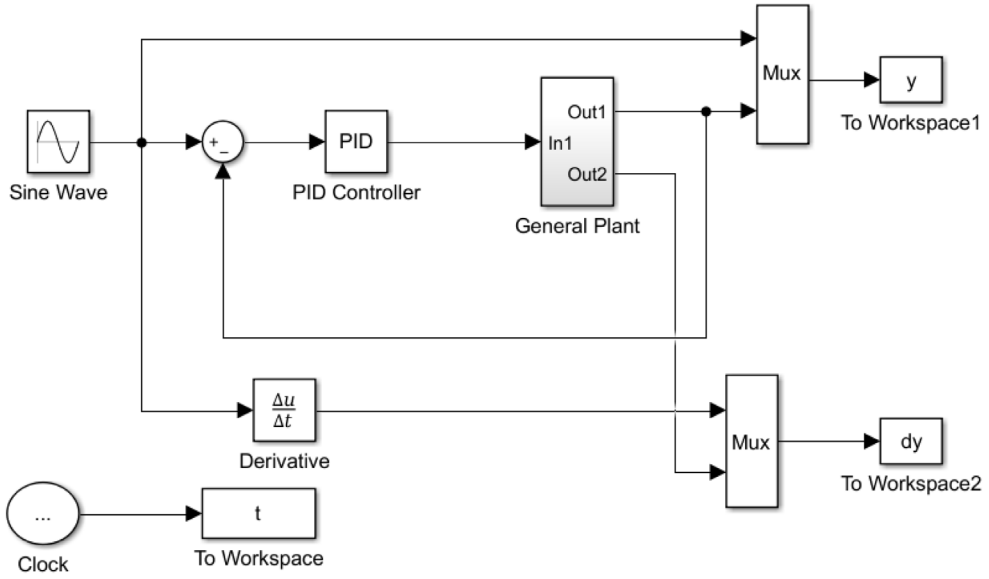

Fig. 7. Simulation model of the two-mass servo PID control system.

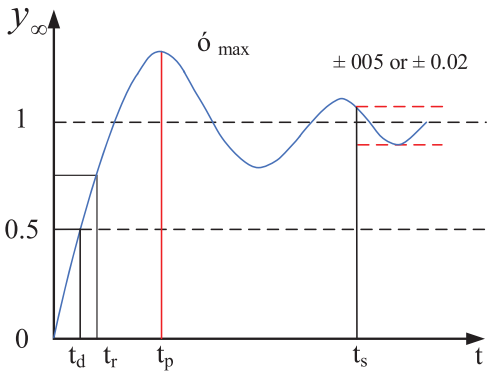

Fig. 8. Response curve of the servo system under the step signal.

order system composed of servo feed system and mechanical system, the overshoot $\sigma$and adjustment time t_s are expressed in equations (12) [16].

In equation (12), it can be seen that in the high-order systems, the overshoot is related to the position of

$$\begin{cases} \sigma = \dfrac{\prod_{i=3}^{n} |si|}{\prod_{i=3}^{n} |s1 - si|} \\ ts \approx \dfrac{3}{\xi \omega n} \end{cases} \tag{12}$$

pole-zero of transfer function, and the adjustment time t_s is inversely proportional to the inherent frequency ω_n and the damping ratio ξ. In this paper, the Simulink is emploied to simulate high-order systems. Under the initial condition, the loading inertia ratio n is modified by changing the loading inertia of the servo feed system, the unit step response curves of the servo system under the single-axis driving and double axes driving are shown in Figure 9.

From Figure 9, it can be seen that with the increase of the load inertia ratio n, the maximum overshoot of the servo system gradually increases, both the rising time *tr* and the adjustment time *ts* increase, the response speed and the stability of the servo system decreases. In addition, under the same load inertia condition, the response speed of the double-axes driving is faster, and the overshoot is relatively small. Therefore, in the initial condition, in order to make the system response quickly and stable, the preferred inertia ratio is the n $\leq$ 3.

3.2 Influence on the gain upper limit of servo system

The position loop gain is closely related to the fast responsiveness, stability and positioning accuracy of the servo system. The higher the upper limit of the position loop gain, the faster the dynamic response and the smaller the steady-state errors of the servo system. However, if the gain of the position loop is too large, the oscillation will occur. In this connection, the double-axes driving control model is simplified as the position loop transfer function, which is shown in Figure 10.

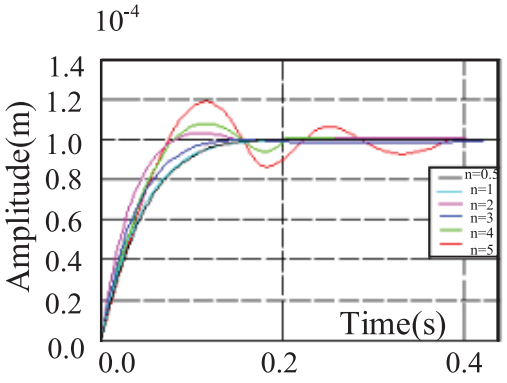

(a) Single-axis driving

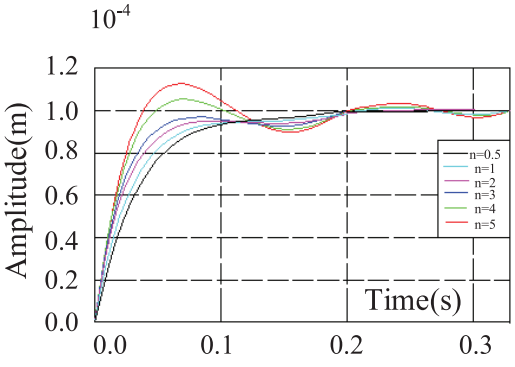

(b) Double-axes driving

Fig. 9. Unit step response curves under the single-axle. driving and double-axle drivingg.

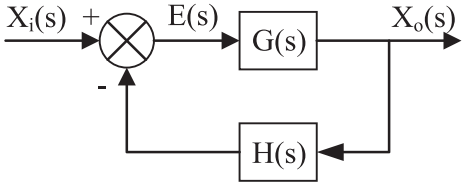

Fig. 10. Position loop transfer function of the simplified double-axes driving control model.

The steady-state errors is defined as $e_{ss} = \mathrm{lime}(t)$, and transformed by Laplace transformation, which is as shown in equations (13), (14), (15) and (16), respectively..

$$ess = \lim e(t) = \lim sE(s) \tag{13}$$

$$E(s) = Xi(s) - H(s)X0(s) \\ = Xi(s) - H(s)G(s)E(s) \tag{14}$$

$$E(s) = \frac{1}{1 + G(s)H(s)} Xi(s) \tag{15}$$

$$ess = \lim_{s\to 0} s \frac{1}{1 + G(s)H(s)} Xi(s) \tag{16}$$

If $G_k(s)$ is set as the open-loop transfer function of the servo system, which can be expressed as equation (17).

$$Gk(s) = G(s)H(s) = \frac{K\prod_{i=1}^{m}(Tis + 1)}{s^v \prod_{j=1}^{n-v}(Tjs + 1)} \tag{17}$$

where, v is the number of series integration link. Define $v = 0, 1, 2$, corresponding to the type 0, type I and type II, respectively, which can be expressed as equation (18) [17].

$$G0(s) = \frac{\prod_{i=1}^{m}(Tis + 1)}{s^v \prod_{j=1}^{n-v}(Tjs + 1)} \tag{18}$$

Then

$$\lim_{s\to 0} G0(s) = 1 \tag{19}$$

$$Gk(s) = G(s)H(s) = \frac{KG0(s)}{s^v} \tag{20}$$

$$ess = \lim_{s\to 0} sE(s) \\ = \lim_{s\to 0} s \frac{Xi(s)}{1 + G(s)H(s)} = \lim_{s\to 0} \frac{s^{v+1}Xi(s)}{KG0(s) + s^v} \approx \lim_{s\to 0} \frac{s^{v+1}Xi(s)}{K} \tag{21}$$

From equation (21), it can be seen that the magnitude of the servo system steady-state errors is related to the type of system, mechanical structure parameters, servo parameters, system equivalent gain and input signal. By changing the load inertia and adjusting the gain of the system position loop, taking the no overshoot of the position loop as the constraints of step response performance, the relationship between the load inertia ratio and the gain upper limit of position loop under the single-axis driving and double-axes driving are studied, and the simulation results are shown in Figure 11.

It can be seen that with the loading inertia ratio gradually increasing, the gain upper limit of position loop decreases and the descending speed decreases, the static errors of the system increases and the dynamic response speed of the system decreases both in single-axis driving and double-axes driving. In addition, even if the load inertia ratio is same, the gain upper limit of the position loop of double-axes driving is slightly higher than that of the single-axis.

3.3 Influence on the servo system following errors

Due to inertia, the output of CNC machining servo system lags behind input to some extent, and the difference between them is following errors. The servo system following errors are the proportional to the speed command and inversely proportional to the gain of the position loop. By changing the loading inertia, taking the sine signal as the position input signal and the position loop gain as the servo system control parameters, the change laws of the servo system following errors with different loading inertia ratios n under the single-axis driving and double-axes driving are simulated and analyzed, and the simulation results are shown in Figure 12.

As illustrated in Figure 12, with the increase of the loading inertia ratio n, the servo system following errors increases, however, the following accuracy of the servo system decreases, and the following errors changes together with the input signal speed. In addition, under the same loading inertia, compared with the single-axis driving system, the double-axes driving system can obtain higher position gain and relatively smaller tracking errors.

3.4 Influence on the interference-free stiffness of servo system

The interference-free dynamic stiffness of the servo system is the unit output angle caused by the feed mechanism (i.e. ball screw) under the different frequency interference signals, which is shown in equation (22).

$$K(j\omega)|_n = Tg(j\omega)/\theta_{out}(j\omega). \tag{22}$$

It reflects the ability of the servo system to resist position errors under the influence of the external interference signals. In this paper, the anti-interference dynamic stiffness of the servo system under different load inertia ratios is shown in Figure 13.

As shown in Figure 14, the anti-interference stiffness of the system decreases with the increase of the inertia ratio in the low frequency range and increases together with the inertia ratio in the medium and high frequency, which having a better inhibition action to the high frequency disturbance. In addition, under the same load inertia, the anti-interference stiffness of double-axes driving system is higher than that of the single-axis driving. So, in the initial condition, in order to improve the interference-free dynamic stiffness of the servo system, the preferred inertia ratio is $3 \le n \le 5$.

3.5 Influence on the closed loop frequency characteristics of servo system

The closed-loop frequency characteristics of the servo system are described as equation (23).

$$G(j\omega)|n = yin(j\omega)/yout(j\omega) \tag{23}$$

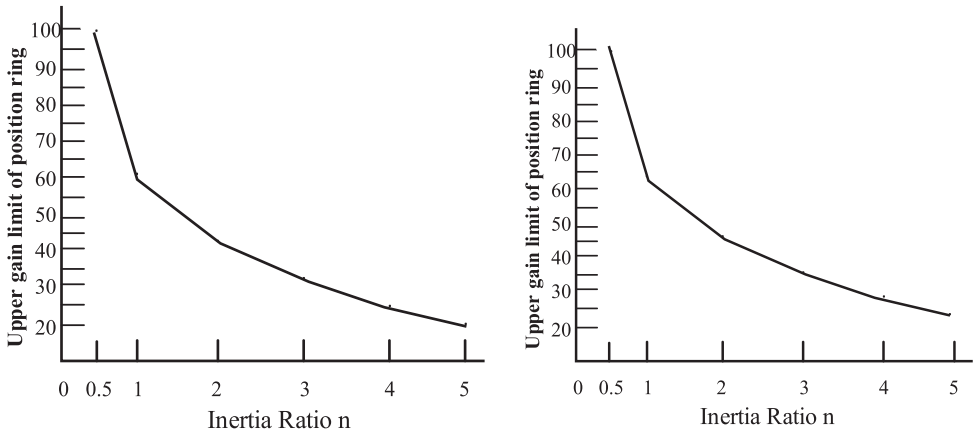

(a) Single-axis driving (b) Double-axes driving

Fig. 11. Relationship between the load inertia. ratio and the gain upper limit of position loop.

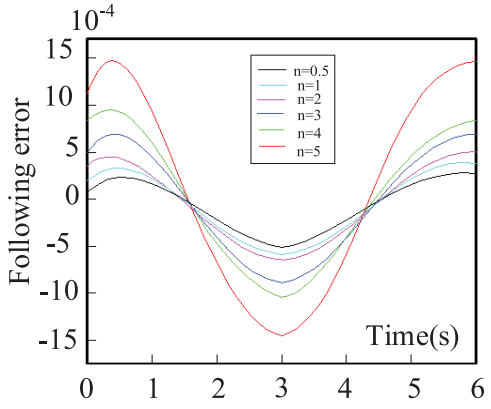

(a) Single-axis driving

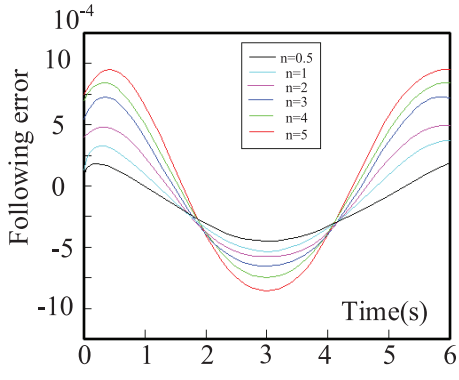

(b) Double-axes driving

Fig. 12. Change laws of the servo system following errors with different loading inertia ratios n under the single-axis driving and double-axes driving.

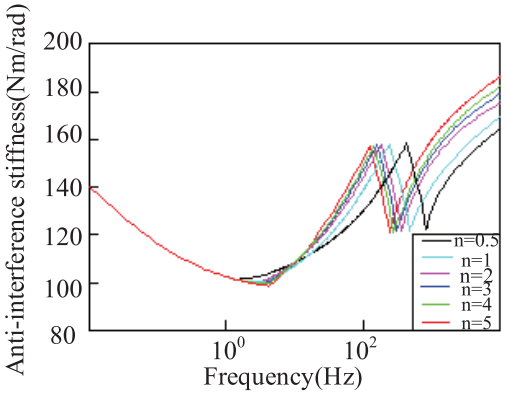

(a) Single-axis driving

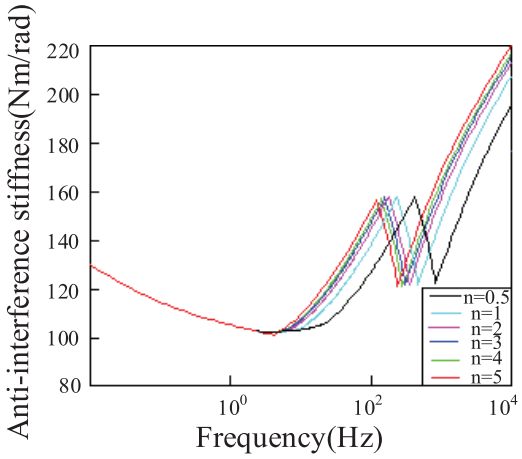

(b) Double-axes driving

Fig. 13. Anti-interference dynamic stiffness of the servo system under different load inertia ratios.

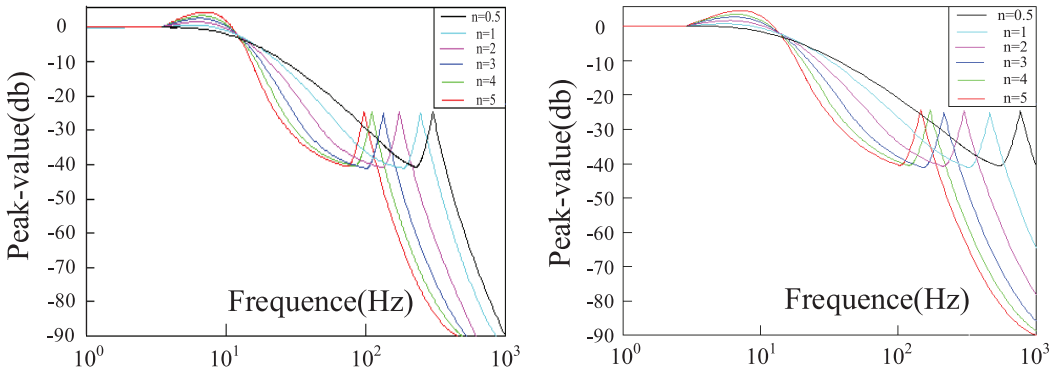

Fig. 14. Amplitude-frequency characteristic curve of the servo system under the different load inertia ratios.

The closed-loop frequency characteristics of the servo system position loop under the different loading inertia ratios are calculated, and the amplitude-frequency characteristic curve of the servo system is shown in Figure 14.

As illustrated in Figure 14, when the inertia ratio is $0.5 \leq n \leq 2$, the control bandwidth of the double-axes driving increases together with the load inertia ratio, while when the inertia ratio is $2<n \leq 5$, the control bandwidth of the double-axes driving decreases with the increase of the load inertia ratio. In addition, with the increase of load inertia, the resonance frequency of the system decreases gradually, and the position loop of the double-axes driving system can obtain a higher control bandwidth at the same inertia ratio. Therefore, for the servo system with large load inertia, in order to have a high control bandwidth and avoid resonance, the speed regulation performance of the system will be reduced. It is preferred that the inertia ratio of the double-axes driving system be less than $n< 2$ and that of the single-axis driving system be less than $n < 3$.

4 Influence of the inertia ratio on the servo system contour errors

The CNC servo system accurately controls the speed and position of each axis according to the command signals to obtain the different motion trajectories. Due to the influence of the mechanical structure of the system on the steady-state and dynamic performance of the servo system, the contour errors are inevitably generated during the synchronous driving process of each axis, which thereby affects the machining accuracy of the CNC machine. In this connection, it is essential to analyze the influence of the inertia ratio on the servo system contour errors.

4.1 Influence on the linear contour errors of servo system

Perfect inertia matching between the X-axis and Z-axis is significant to guarantee the excellent gear grinding quality. Thus, it is necessary to analyze the influence of inertia ratio on the servo system contour errors during the synchronous driving of X-axis and Z-axis. Assuming the input speed of synchronous driving of X-axis and Z-axis is ν, the angle between ν and the positive X-axis is θ, the theoretical desired positions of the two axes are shown in equation (24).

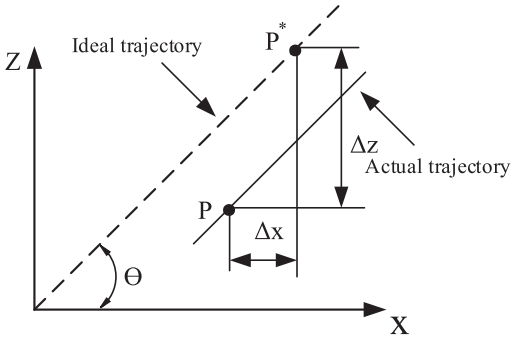

Fig. 15. Schematic diagram of contour errors of the linear motion trajectory.

$$\begin{cases} xi(t) = (\nu \cos\theta)t \\ zi(t) = (\nu \sin\theta)t \end{cases} \tag{24}$$

During the liner motion of the CNC machine, the contour errors of the synchronous driving trajectory of the two axes is generated due to the following errors between the two axes, and the schematic diagram is shown in Figure 15.

As shown in Figure 15, X-axis and Z-axis move along a straight line in the X−Z plane. The angle between the theoretical desired trajectory and the positive X-axis is θ, P^* is the theoretical position and P is the corresponding actual position. The following errors of X-axis and Z-axis are $\triangle x$ and $\triangle z$, respectively, and the contour errors ε can be expressed in equation (25).

$$\varepsilon = \Delta z \cos\theta - \Delta x \sin\theta \tag{25}$$

The following errors of two axes are recorded in equation (26).

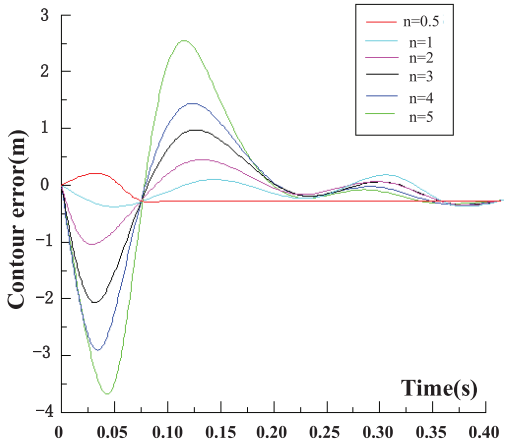

Fig. 16. Servo system linear trajectory contour errors when changing X-axis inertia ratio separately.

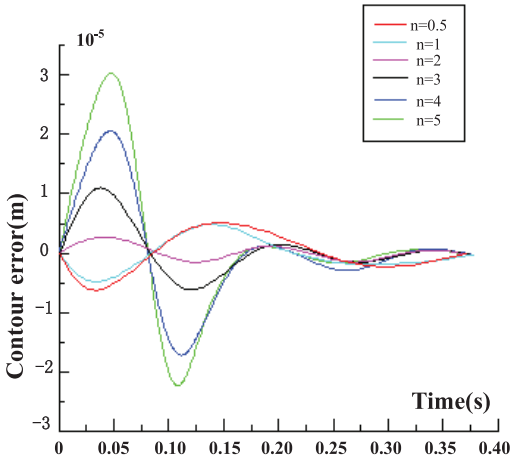

Fig. 17. Servo system linear trajectory contour errors when changing Z-axis inertia ratio separately.

$$\begin{cases} \Delta x = Px^* - Px \\ \Delta z = Pz^* - Pz \end{cases} \tag{26}$$

Substitute equation (26) into equation (25), then ε can be obtained, which is shown in equation (27).

$$\begin{aligned} \varepsilon &= (Pz^* - Pz)\cos\theta - (Px^* - Px)\sin\theta \\ &= (Pz^*\cos\theta - Px^*\sin\theta) - (Pz\cos\theta \\ &\quad - Px\sin\theta) \end{aligned} \tag{27}$$

For the ideal liner trajectory, there

$$Pz^*\cos\theta - Px^*\sin\theta = 0 \tag{28}$$

So, combined with equation (28), equation (27) can be simplified to equation (29).

$$\varepsilon = Px\sin\theta - Pz\cos\theta \tag{29}$$

Set other structural parameters be invariant, the input speed signal ν is 30 mm/s, the angle θ between ν and the positive X-axis is 45°, only change the load inertia ratio, and the linear contour errors change rules of the servo system is simulated and analyzed. Maintaining Z-axis inertia ratio unchanged, changing X-axis load inertia ratio, the simulated liner contour errors is shown in Figure 16.

From Figure 16, it can be seen that the linear contour errors of X-axis fluctuate greatly during the acceleration phase of linear motion and tend to stabilize gradually within 0.35 s. When n = 0.5, the contour errors are mainly positive (maximum:2.4×10^{-5}). When load inertia ratio is within $1 \leq n \leq 5$, the fluctuation degree of the line contour errors and the maximum contour errors increase together with the inertia ratio. When the load inertia ratio n = 5, the max contour errors is -3.76×10^{-4}. So, it is preferred that the load inertia ratio of the double-axes driving servo system X-axis is taken as $n \leq 2$.

Similarly, Maintaining X-axis inertia ratio unchanged, changing Z-axis inertia ratio, the simulated linear contour errors is shown in Figure 17.

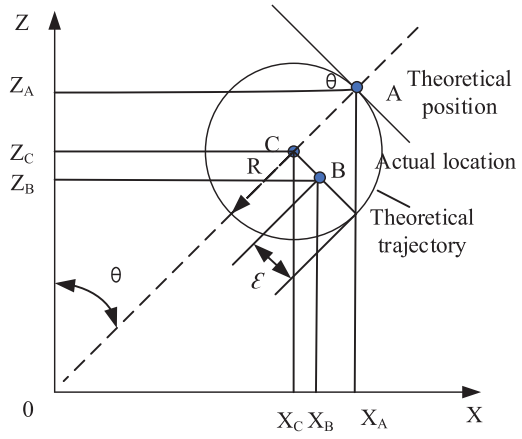

Fig. 18. Schematic diagram of the contour errors of the arc.

As seen Figure 17, the linear contour errors of Z-axis fluctuate greatly and tend to be stable over time during the acceleration stage of linear motion. Whereas, when $0.5 \leq n \leq 1$, the maximum contour errors decreases with the increase of load inertia, but the difference is not obvious. When $2 \leq n \leq 5$, the contour errors increases together with the load inertia [18, 19]. So, the load inertia ratio of the double-axes driving servo system Z-axis is preferred $0.5 \leq n \leq 2$ to realize the excellent linear machining accuracy.

4.2 Influence on the circular contour errors of servo system

During the circular motion of the CNC machine, double-axes position commands are set as equation (30).

$$\begin{cases} xi(t) = R\sin\left(\dfrac{\nu}{R}t\right) \\ zi(t) = R\cos\left(\dfrac{\nu}{R}t\right) - R \end{cases} \tag{30}$$

where, R is the arc radius, ν/R is the angular velocity. In actual motion, contour errors inevitably exist in the circular motion due to the following errors $\triangle x$ and $\triangle z$ of the X-axis and Z-axis, which is shown in Figure 18.

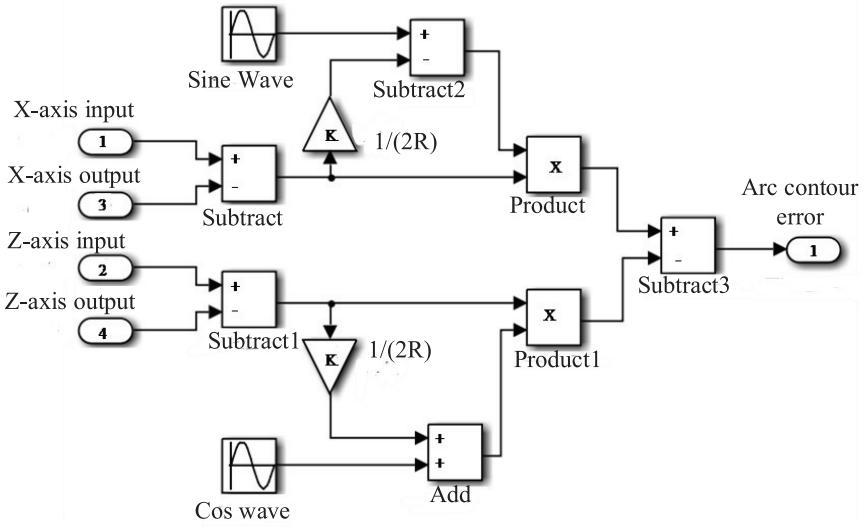

Fig. 19. Computational model of contour errors of circular arc motion.

In Figure 18, θ is the angle between the theoretical reference point A and X-axis, R is the arc radius, $A(A_x,A_z)$ is the theoretical reference point, $B(B_x,B_z)$is the corresponding actual point, $C(C_x,C_z)$is the center of the circular trajectory, then the contour errors ε of the arc trajectory can be expressed in equation (31).

$$\varepsilon = \mathrm{R} - \sqrt{(B\mathrm{x} - C\mathrm{x})^2 + (B\mathrm{z} - C\mathrm{z})^2} \tag{31}$$

The location of actual point B is:

$$\begin{aligned} B\mathrm{x} &= A\mathrm{x} - \Delta\mathrm{x} \\ &= C\mathrm{x} + \mathrm{R}\sin\theta - \Delta\mathrm{x} \end{aligned} \tag{32}$$

$$B\mathrm{y} = A\mathrm{z} - \Delta\mathrm{z} = C\mathrm{z} + \mathrm{R}\cos\theta - \Delta\mathrm{z} \tag{33}$$

Substitute equation (32) and (33) into equation (31), the contour errors ε can be obtained, which is shown in equation (34).

$$\begin{aligned} \varepsilon &= \mathrm{R} - \sqrt{(\mathrm{R}\sin\theta - \Delta\mathrm{x})^2 + (\mathrm{R}\cos\theta - \Delta\mathrm{z})^2} \\ &= \mathrm{R} - \sqrt{\mathrm{R}^2 - 2\mathrm{R}(\Delta\mathrm{x}\sin\theta - \Delta\mathrm{z}\mathrm{R}\cos\theta) + (\Delta\mathrm{x}^2 - \Delta\mathrm{z}^2)} \\ &= \mathrm{R} - \sqrt{1 + \frac{\Delta\mathrm{x}^2 + \Delta\mathrm{z}^2}{\mathrm{R}^2} - 2\frac{\Delta\mathrm{x}\sin\theta - \Delta\mathrm{z}\cos\theta}{\mathrm{R}^2}} \end{aligned} \tag{34}$$

Assuming Δx and Δy are much larger than ε, and R is large enough, equation (34) can be expanded by applying Taylor formula.

$$\begin{aligned} \varepsilon &= \mathrm{R} \\ &- \mathrm{R}\left[1 + \frac{1}{2}\left(\frac{\Delta\mathrm{x}^2 + \Delta\mathrm{z}^2 - 2\mathrm{R}\Delta\mathrm{x}\sin\theta + 2\mathrm{R}\Delta\mathrm{z}\cos\theta}{\mathrm{R}^2}\right) + \cdots\right] \end{aligned} \tag{35}$$

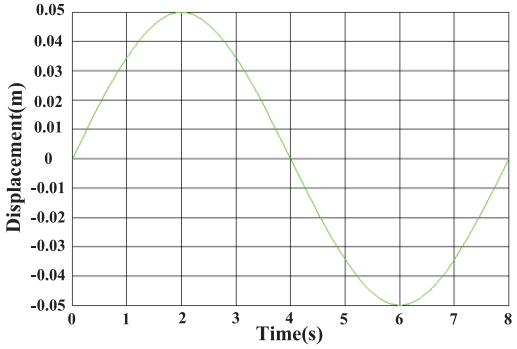

Fig. 20. X-axis input signal.

If higher order items of equation (35) are omitted, equation (34) can be simplified to equation (36).

$$\varepsilon = (\sin\theta - \frac{\Delta\mathrm{x}}{2\mathrm{R}})\Delta\mathrm{x} - (\cos\theta + \frac{\Delta\mathrm{z}}{2\mathrm{R}})\Delta\mathrm{z} \tag{36}$$

For any curvilinear motion, the contour can be infinitely approximated by an arc, which substituting its curvature radius for the arc radius at a certain point. Therefore, the contour errors can be expressed by equation (36) during the double-axes curve synchronous driving. The calculation model built in Simulink is shown in Figure 19.

Change the load inertia ratio and keep other structural parameters unchanged, the circular contour errors change rules of the servo system is simulated and analyzed. The maximum input speed signal $v$is 5 m/min and the arc radius is 0.05 m. The input position command signals of X-axis and Z-axis are shown in Figures 20 and 21.

Maintaining the inertia ratio of one axis unchanged, the circular contour errors of the simulation calculation results is shown in Figure 22. It can be seen that the circular

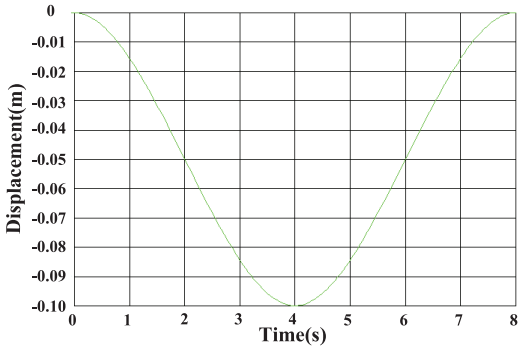

Fig. 21. Z-axis input signal.

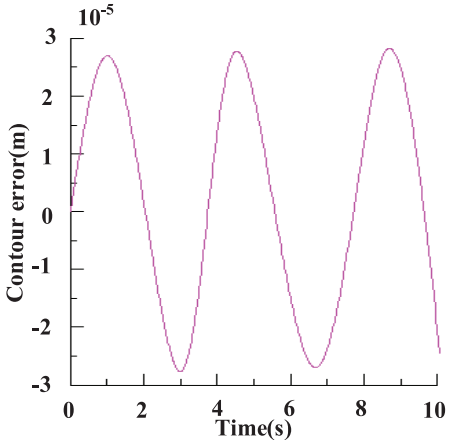

Fig. 22. Simulation calculation results of the circular contour errors.

Fig. 23. Cycloidal gear form grinding.

Fig. 24. Cycloidal gear measuring.

contour errors of CNC machine change periodically during the double-axes arc motion, and the maximum contour errors occurs at the commutating time of each axis. Changes of the inertia ratio have less influence on the arc motion contour errors of servo system.

Therefore, combined with the influence analysis of the inertia ratio on the servo system control performance and contour errors, in order to reduce the linear motion contour errors of the servo system and make the servo system have higher machining accuracy, the precise range of the inertia ratio can be optimized as $0.5 \leq n \leq 2$.

5 Grinding experiment of the cycloidal gear

To verify the rationality of the optimized inertia ratio, the inertia ratio optimization grinding experiments were conducted on the CNC cycloidal gear form grinding machine YK7350B is independently developed by the Gear Manufacturing Henan Engineering Technology Research Center. The tooth profile of the grinded cycloidal gear is measured on Gleason 650 gear measuring machine. The cycloidal gear form grinding is shown in Figure 23, and the cycloidal gear measuring is shown in Figure 24. The measuring results of the cycloidal gear tooth profile before and after the inertia ratio optimized in grinding process are shown in Figures 25 and 26, respectively.

From Figures 25 and 26, it can be seen that the maximum tooth profile deviations of the cycloidal gear before inertia ratio optimized is 0.037288 mm, the minimum tooth profile deviations is −0.017133 mm and the difference between them is 0.020155 mm.

Comparatively, the maximum tooth profile deviations of cycloidal gear after the inertia ratio optimized is 0.019536 mm, the minimum tooth profile deviations is −0.007253 mm and the difference between them is 0.012283 mm. The comparison shows that the cycloidal tooth profile deviations is reduced and satisfied with the requirements of grade 4 accuracy of tooth profile. After optimizing the inertia ratio, the cycloidal gear profile is more stable, the variation range of tooth curve is much less, so as to the roughness of cycloidal gear tooth surface is improved and the tooth surface accuracy is ensured to a certain extent.

6 Conclusion

Through the inertia matching analysis of the CNC cycloidal gear form grinding machine servo system, the two-mass servo driving closed-loop PID control system is constructed. The influence laws of different inertia ratios on the system control performance and the system profile errors are studied and analyzed. The feasibility and practicability of the inertia matching design for the CNC gear form grinding machine

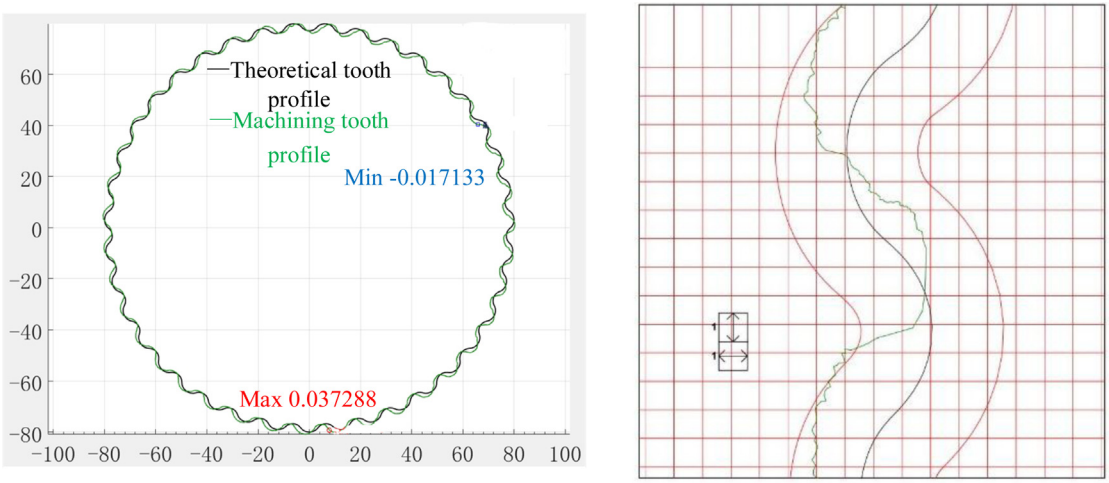

（a）Cross-sectional errors comparison （b）Cycloidal profile

Fig. 25. Measuring results of the cycloidal gear tooth profile before the inertia ratio optimized.

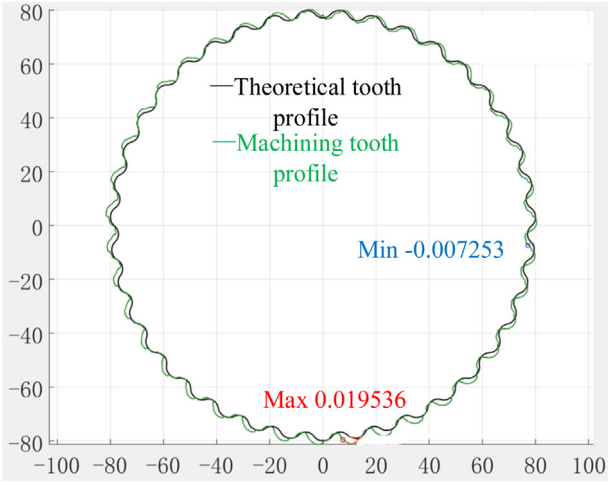

（a）Cross-sectional errors comparison

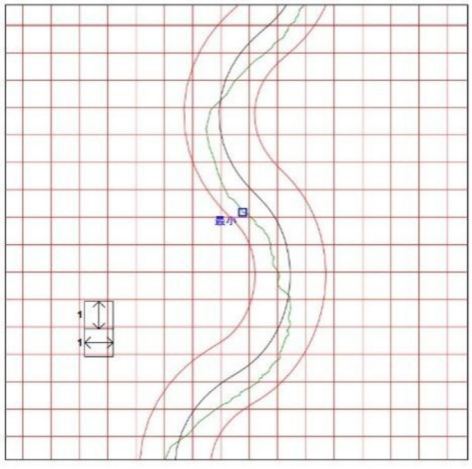

（b）cycloidal profile

Fig. 26. Measuring results of the cycloidal gear. tooth profile after the inertia ratio optimized

servo system is verified by the simulation analysis and machining experiment of different inertia ratios. The main research conclusions are as follows:

– With the increase of the inertia ratio, the response time and stability time of single-axis and double-axes driving systems increase, the following errors of the servo system increases, and the anti-interference stiffness in high frequency band of the servo system increases. Meanwhile, the upper limit of the gain of closed-loop position control of the servo system decreases, the resonant frequency of the system decreases gradually, the fast response speed of the system decreases, the speed regulation performance of the system decreases, and the anti-interference stiffness of the system in low frequency band decreases. Under the same load inertia, the dynamic performance indexes of the double-axes driving system are more superior.
– In the double-axes simultaneous motion process of the CNC cycloidal gear form grinding machine, the increase of the load inertia both X-axis and Z-axis will cause a change in the linear contour errors of the servo system, but it has little influence on the circular contour errors of the servo system. Therefore, in the double-axes CNC machine tool with cross sliding table and other structures, the preferred inertia ratio is $0.5 \leq n \leq 2$, so as to reduce the linear contour errors of servo system and ensure the machining accuracy.
– The inertia matching optimization design method proposed in this paper provides a valuable reference for improving the control performance and contour machining precision of the CNC cycloidal gear form grinding machine servo system, as well as the development of the cycloidal gear machining quality. Strictly speaking, in studying the influence of inertia ratio on the dynamic adjustment performance of the servo system, the model is simplified. The established servo driving model is an idealized model, which without considering the changes in ball screw diameter, stiffness, and other aspects with the load inertia changing. The research results may have some deviations from the actual results,

so the next efforts is to establish a more accurate servo system model and further research on the problem of inertia matching.

Conflict of Interest

The author(s) declared no potential conflicts of interest with respect to the research, authorship and/or publication of this article.

Funding

The author(s) disclosed receipt of the following financial support for the research, authorship, and/or publication of this article. This work was supported by the National Key R&D Program of China (No. 2020YFB2006800) and National Natural Science Foundation of China (No. 51405135, No. 51775171).

References

[1] R.W. Armstrong, Load to motor inertia mismatch: unveiling the truth, presented at Proceedings of Drives Control Conference, Telford, England, 1, 1998
[2] S.H. Li, Z,G. Liu, Adaptive speed control for permanent-magnet synchronous motor system with variations of load inertia, IEEE Trans. Ind. Electron. **56**, 3050−3059 (2009)
[3] G. Zhang, J. Furusho, Speed control of two-inertia system by PI/PID control, IEEE Trans. Ind. Electron. **47**, 603−609 (2000)
[4] G.W. Younkin, W.D. McGlasson, Considerations for low-inertia ac drives in machine tool axis servo applications, IEEE Trans. Ind. Applic. **27**, 262−267 (1991)
[5] G. Pritschow, A comparison of linear and conventional electromechanical dives, Ann. CIRP **47**, 541−548 (1998)
[6] J. Moscrop, C. Cook, P. Moll, Control of servo systems in the presence of motor-load inertia mismatch, paper presented at Proceedings of 27th Annual Conference of the IEEE Industrial Electronics Society,xx 2001, pp. 351−356
[7] K. Benath, J. Schuetzhold, W. Hofmann, Advanced design rules for the energy optimal, Motor-gearbox combination in servo drive systems, paper presented at Proceedings of International Symposium on Power Electronics, Electrical Drives, Automation and Motion (SPEEDAM), Italy, 2014, pp. 94–99
[8] P. Boscariol, R. Caracciolo, D. Richiedei, Does inertia matching imply energy efficiency? paper presented at Proceedings of 1st IFToMM for Sustainable Development Goals Workshop (I4SDG), Electr. Network **108**, 282–289 (2021)
[9] Z.F. Shao, X.Q. Tang, X. Chen, L.P. Wang, Research on the inertia matching of the Stewart parallel manipulator, Robot. Comput. Integr. Manuf. 28, 649–659 (2012)
[10] T. Zhang, D. Zhang, Z. Zhang, M. Muhammad, Investigation on the load-inertia ratio of machine tools working in high speed and high acceleration processes, Mech. Mach. Theory **155**, 104093 (2021)
[11] Y.F. Zhang, L. Zhou, SW. Jang, Inertia matching analysis in servo drive of heavy duty CNC machine tool, Combin. Mach. Tool Automatic Mach. Technol. **05**, 5−8 (2017)
[12] H. Liu, Y. Huang, W.H. Zhao, Comprehensive analysis and design of load inertia ratio of CNC machine tool feed system under multi-factor coupling conditions, J. Mech. Eng. **50**, 108−113 (2014)
[13] L. Yuan, M.J. Xu, Z.X. Wu, J. Xu, Dual motor synchronization control method based on load inertia matching, Motor Control Applic. **36**, 43−49 (2019)
[14] Y. Wang, X. Yu, L. Wu, Selection and analysis of servomotor for three-axis transmission system in CNC machine tool, Adv. Mater. Res. **760−762**, 1148–1153 (2013)
[15] X. KeMing, L. GuoYong, Z. DaZhong, Modern Control Theory, Tsinghua University Press, Beijing, China, 2003, pp. 13−20
[16] L. YouShan, Automatic Control Principle, National Defense Industry Press, Beijing, China, 2005, pp. 11−18
[17] Y. ShuZi, Y. KeChong, Fundamentals of Mechanical Engineering Control, Huazhong University of Science and Technology Press, Wuhan, China, 2011, pp. 26−37
[18] C. Li, B. Yao, X. Zhu, Q. Wang, Dual drive system modeling and analysis for synchronous control of an H-type gantry, paper presented at Proceedings of IEEE/ASME International Conference on Advanced Intelligent Mechatronics (AIM), Busan, South Korea, 2015, pp. 214−219
[19] K. Erkorkmaz, Y. Altintas, High speed CNC system design. Part II: modeling and identification of feed drives, Int. J. Mach. Tools Manuf. **41**, 1487−1509 (2001)

Cite this article as: J. Li, J. Su, M. Gao, D. Zhao, L. Zhang, D. Wang, F. Shi, Inertia matching of CNC cycloidal gear form grinding machine servo system, **24**, 31 (2023)